LACE: Loss-Aware Constellation Design for Global-Scale Entanglement Distribution

Huayue Gu, Runzhe Mo, Quntao Zhuang, Ruozhou Yu

***Abstract*—Quantum networks are essential to establishing long-distance entanglements for many advanced quantum applications. Recent breakthroughs have opened up the possibility of creating a satellite-assisted global-scale quantum network. This paper proposes LACE, a Loss-Aware Constellation Design framework for a new type of satellite-assisted *passive-optical* quantum networks. The goal of LACE is to ensure lowest possible worst-case loss for ground-to-ground entanglement distribution with a fixed number of satellites. Considering high photon loss and beam propagation, we first develop a detailed loss model, incorporating factors such as beam propagation and diffraction, atmospheric turbulence, and beam truncation during end-to-end entanglement distribution. We then design an algorithm to estimate the end-to-end loss given a specific network constellation design, and propose a constellation design framework to find a suitable constellation design with as low end-to-end loss as possible. Using LACE, we explore diverse satellite constellations under practical constraints, which reveals critical insights into how network parameters and link connectivity affect end-to-end entanglement loss. Notably, we find that a constellation with 25 orbits and 32 satellites per orbit with an altitude 550 km can establish a channel with approximately 30 dB loss, corresponding to only 150 km of ground fiber distance, between ground stations separated by nearly 20,000 km. These insights provide concrete guidance for future constellation design, paving the way toward global-scale entanglement distribution.**

***Index Terms*—Entanglement distribution, constellation design, propagation model, LEO satellites, quantum network.**

I. Introduction

In recent years, the development of a global-scale quantum network has become increasingly critical for enabling entanglement distribution across long distances, serving as the foundation for emerging quantum applications such as quantum key distribution (QKD) [3], distributed quantum computing (DQC) [7], and quantum sensing [27], [28]. However, a major obstacle to establishing a long-range entanglement with a photon-based quantum network is the inevitable photon loss in the transmission process. For example, direct photon transmission through optical fibers is practically constrained to a few hundred kilometers, as the optical fiber loss increases exponentially as the distance increases [22]. Additionally, unlike classical signals, quantum states cannot be copied or amplified without adding noise due to the no-cloning theorem [25]. Therefore, typical noise control schemes in classical communication are not applicable in a quantum network.

To overcome the limitation in long-distance transmission, the first-generation quantum network has been proposed [11]. End-to-end entanglements are established through a sequence of entanglement generation and entanglement swapping across multiple repeaters. Despite their promise, quantum repeater networks still face several critical challenges that hinder their practical deployment, especially in limited quantum memories, inefficient measurement devices, and exponential photon loss with increasing distance in optical fiber connection [10], [17].

In contrast, recent advances in satellite-based quantum communication have provided notable successes [20]. In particular, quantum satellites such as Micius have successfully demonstrated the entanglement distribution over distances greater than 1,200 km through free-space optical links in the actual experiment [26]. Despite the promises, the feasibility of building and operating a satellite-assisted global quantum network has not been validated. A single satellite is not sufficient to cover the entire globe (see Sec. III). Meanwhile, building an entire quantum satellite network faces numerous open problems, ranging from near-term quantum device availability and resource constraints to detailed modeling of in-space propagation and performance/cost analysis.

This paper introduces a novel Loss-Aware Constellation Design framework for satellite-assisted quantum networks, named **LACE**, aimed at achieving global-scale entanglement distribution with minimal worst-case loss. Uniquely, LACE is based on a new quantum satellite network architecture, which utilizes only passive in-orbit optical instruments and no active quantum devices such as repeaters or memories in space [10], [12]. Our main contributions are as follows:

- We propose a Loss-Aware Constellation Design framework to support global-scale entanglement distribution. To the best of our knowledge, this is the first work to explore constellation design with a passive-optical quantum network architecture.
- We develop a comprehensive analysis and characterization of the photon transmission loss model, analyzing the impact of turbulence loss in uplink and downlink, diffraction losses between satellites, and beam truncation.
- We then design an algorithm to estimate the end-to-end loss, and propose a constellation design framework to determine the parameters for the lowest worst-case loss.
- We explore diverse satellite constellations under different constraints with extensive simulations, and describe critical insights that will guide the future development of quantum satellite network constellations.

Organization. §II introduces background. §III provides quantum network preliminaries. §IV characterizes the photon transmission loss model. §V presents the end-to-end loss estimation algorithm and constellation design framework for the worst-

Gu and Yu ({hgu5, ryu5}@ncsu.edu) are with NC State University, Raleigh, NC 27606, USA. Mo and Zhuang ({runzhemo, qzhuang}@usc.edu) are with University of Southern California, Los Angeles, CA 90007, USA. Gu and Yu were supported in part by NSF grant No. 2350152. Mo and Zhuang were supported in part by NSF grant No. 2350153. The information reported herein does not reflect the position or the policy of the funding agencies.

case loss. §VI shows evaluation results. §VII is the conclusion.

II. Background and Related Work

Existing works primarily focused on terrestrial quantum repeater networks, especially in network optimization with different objectives. However, the reliance on repeaters hinders the deployment for global-scale entanglement distribution.

Compared to terrestrial repeater networks, quantum satellite networks show many advantages and potential. For instance, light experiences almost zero loss in near-vacuum conditions, and is mostly affected by beam diffraction that can be realistically captured or controlled. Compared to the 0.2 dB/km fiber loss on the ground, space presents significantly lower loss over distance exceeding several hundred kilometers, as demonstrated in existing long-distance experiments [26]. The initial idea was to consider a single satellite as a relay station for swapping and then serve two remote nodes in a double-uplink architecture. Panigrahy *et al.* [21] focused on distributing entanglements to remote ground station pairs while deploying entanglement sources on satellites using a double-downlink configuration. Boone *et al.* [5] studied entanglement distribution in ground stations placed only on the equator. Khatri *et al.* [17] then designed a quantum internet consisting of a constellation of orbiting satellites with continuous coverage. However, all regard satellites as entanglement sources and they ignore the fact that the restricted energy budget and payload constraint of deploying such complex devices on the satellites.

Inspired by recent breakthroughs in direct quantum communication with passive light guides [10], [15], entangled photons can be transmitted directly from one to the other with a sequence of lenses, eliminating the need for quantum memories and measurement devices aboard. Numerical simulations show promising results with the approach, both on the ground [15] and in space [10]. Especially in space, the loss can remain relatively low over long distances under ideal free-space propagation, offering advantages over fibers. However, these works have not yet addressed the network constellation design while considering continuous beam propagation. Motivated by these, this paper proposes a novel satellite-assisted constellation framework specifically tailored for quantum networks, aiming to effectively achieve global-scale entanglement distribution.

III. Quantum Network Preliminaries

In this paper, we focus on distributing maximally entangled bipartite quantum states between remote ground stations. We restrict our study to bipartite entangled states, since more complex multipartite entangled states can be constructed from bipartite entanglement distributed among multiple parties [14].

A. Entanglement Distribution via a Passive-Optical Network

Entanglement generation: To enable quantum information exchange between two remote ends, an entanglement source to continuously generate entangled photon pairs is required. Common methods include spontaneous parametric down-conversion (SPDC) [18] and four-wave mixing [19]. While entanglement sources can be placed either on the ground or satellites, challenges such as stability requirements, precise alignment, and high-power laser demands make space deployment difficult.

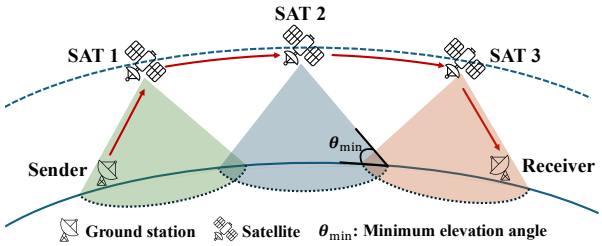

Fig. 1: Entanglement transmission among satellites.

Therefore, deploying entanglement generation sources on the ground is comparatively a more practical and feasible choice.

Entanglement transmission: Instead of the probabilistic process of entanglement generation and swapping in a ground repeater network, entanglement transmission among satellites is more straightforward. Each satellite is equipped with adjustable lenses designed to reflect or refract incoming photons, directing them to subsequent satellites or ground receivers. A sequence of these satellite-mounted lenses forms a direct light path from sender to receiver, as shown in Fig. 1.

B. Satellite Coverage

To determine whether entangled photons can be transmitted between ground stations and satellites, we begin by analyzing the coverage area of a satellite. In particular, a single satellite can only cover a limited portion of the Earth's surface, depending on its altitude and the minimum elevation angle required by the ground stations [8]. We represent the satellite's coverage area as a spherical cap on the Earth's surface following [8]:

$$S_{\text{cov}} = 2\pi R_{\text{e}}^2 \left(1 - \cos(\varphi)\right), \tag{1}$$

where

$$\varphi = \arccos\left(\frac{R_{\text{e}}}{R_{\text{e}} + h} \cos\theta_{\min}\right) - \theta_{\min}, \tag{2}$$

and φ is the angular radius of the coverage circle, h is the altitude, R_{e} is the Earth radius and $\theta_{\min}$ is the minimum elevation angle. The minimum elevation angle, defined as the minimum angle above the horizon required for a ground station to establish a reliable link with a satellite, significantly affects the size of the satellite's visible region. In Fig. 1, as $\theta_{\min}$ increases, the observable surface area decreases significantly, further limiting the region where reliable optical links can be established between ground stations and satellites.

C. Network Model

Formally, we consider a satellite network $G = (V, E)$ as an undirected graph consisting of LEO satellites in multiple orbits, in which V is the set of satellites and E is the set of inter-satellite links (ISLs). The connection of ISLs depends on the lens orientation and field-of-view limitations of satellites, which give rise to different connection strategies (see Sec. VI).

We define $\mathcal{P}$ as the number of orbital planes and $\mathcal{N}$ as the number of satellites in each orbit, and the total number of satellites $\mathcal{V} = \mathcal{N} \times \mathcal{P}$. We define h as the altitude of satellites, with the assumption that all satellites share the same altitude.

To analyze end-to-end entanglement distribution, we model each beam route as a path consisting of a sequence of optical links between ground stations (GSes) and satellites (SATs). A path begins at a GS, traverses one or more SATs, and ends at

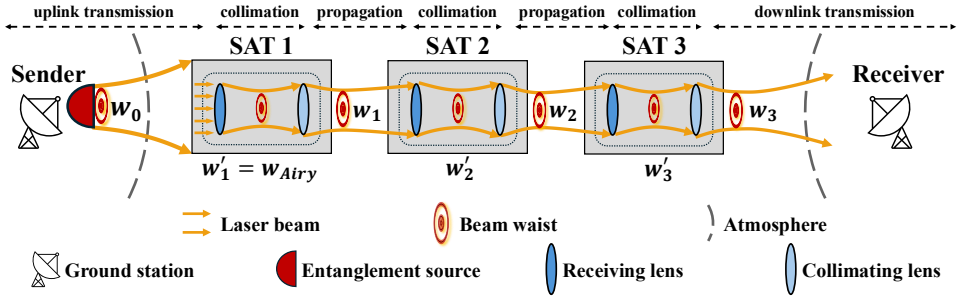

Fig. 2: Beam propagation between a ground station pair.

the other GS. Each link in the path, either a ground-satellite link (GSL) or an ISL, has a transmission efficiency, representing the fraction of photon power successfully transmitted across that segment. Notably, the efficiency evolves dynamically based on the beam state inherited from the previous hop, including beam waist and propagation distance. Consequently, the end-to-end loss must be computed sequentially (see Sec. IV). Besides, the availability of these links, also changes over time due to satellite motion, further changing feasible paths and the end-to-end loss. Considering satellite motion follows deterministic and predictable orbital patterns, it is possible to estimate end-to-end loss by average or by taking the maximum over many snapshots of the satellite networks. Hence, in theoretical modeling, we consider a fixed snapshot of the network.

Instead of focusing on entanglement distribution rate or fidelity, which typically assume each operation as an independent process, we study LACE using transmission loss as the primary metric, as it directly captures the continuous evolution of beam propagation. To evaluate how well a given constellation supports this distribution, It is essential to understand how photons propagate through the network and how transmission loss accumulates along each link, which is explained below.

IV. LACE: Beam propagation Model

In a photon-based quantum network, the predominant bottleneck is the inevitable photon loss during transmission, which is tied to the satellite constellation. For instance, the atmospheric loss during ground-to-satellite transmission depends on the satellite altitude, and inter-satellite diffraction loss varies with the physical separation between satellites. These dependencies emphasize the need for a general loss model that captures how constellation design affects overall transmission loss.

A. Uplink/Downlink Photon Transmission

To establish an entanglement between two ground stations, the sender generates an entangled photon pair with self-equipped entanglement sources and forwards one photon of the pair to the receiver through a series of satellites, as shown in Fig. 2.

During this process, it involves two direct ground-to-satellite links: an uplink from the sender to the entry satellite, and a downlink from the exit satellite to the receiver. The uplink experiences significantly higher turbulence loss compared to the downlink, due to two primary factors. First, in uplink transmission, the beam propagates upward through the turbulent atmosphere, which extends up to around 20 km. Atmospheric turbulence causes beam wandering and broadening [4], effectively increasing the beam divergence early in its path. After exiting the turbulent boundary layer, the already broadened beam continues to propagate for several hundred kilometers toward the satellite, resulting in substantial diffraction loss. Second, practical limitations on the satellite payload restrict the size of receiving lens, which further constraints the efficiency for the uplink beam [10]. In contrast, during the downlink transmission, the beam only encounters turbulence near the end of its path and remains tightly focused during the majority of its propagation, so the turbulence-induced broadening in downlink transmission is much less significant. In this case, we model the uplink loss as a combination of turbulence and diffraction, while for the downlink, we consider diffraction loss only.

We assume the light beam is a Gaussian beam with an initial beam waist of w_0. Due to diffraction, such a beam diverges as it propagates away from its waist, which is defined as the location along the optical axis where the beam reaches its minimum width. In uplink, the size of the beam spot at the satellite can be quantified by the long-term beam width w_{LT} as [9], [10]

$$w_{\mathrm{LT}}^2(z) = w_0^2\left(1+(\frac{z}{z_{\mathrm{R}}})^2\right) + 2\left(\frac{4z}{kr_0}\right)^2, \tag{3}$$

where w_0 is the initial beam width, z is the propagation distance, and $z_{\mathrm{R}} = \pi(w_0^2/\lambda)$ is the Rayleigh range, $k = \frac{2\pi}{\lambda}$ and r_0 is the Fried parameter for the uplink [13]

$$r_0 = \left[0.42k^2\int_0^z C_n^2(z')(\frac{z-z'}{z})^{\frac{5}{3}}dz'\right]^{-\frac{3}{5}}, \tag{4}$$

where $C_{\mathrm{n}}(h)$ is the refractive index structure constant [2], [24]

$$C_{\mathrm{n}}^2(h) = 0.00594\left(\frac{v}{27}\right)^2 h^{10}\left(10^{-50}\right)e^{(-h/1000)} + 2.7\times10^{-16}e^{-h/1500} + Ae^{(-h/100)} \tag{5}$$

with $A = 1.7\times10^{-14}$ and $v = 21m/s$. This $C_{\mathrm{n}}(h)$ profile follows the H-V 5/7 model, which is a widely-used estimation in turbulence analysis [24]. Notice that when estimating the uplink r_0 in Eq. (4), we integrate through the whole optical length, i.e., from sender to the satellite (several hundreds of kilometers) instead of ending at the atmosphere (about 20 km), and therefore the resulting w_{LT} is a high bound estimation [4].

We then define ground-to-satellite link efficiency η_{gs} to quantify the ratio of received power at the satellite to the transmitted power from the sender. The portion of the beam that is beyond the receiving lens's size will be truncated.

$$\eta_{\mathrm{gs}} = \eta_0\left(1-\exp\left(-2\left(\frac{\rho_{\mathrm{r}}}{w_{\mathrm{LT}}}\right)^2\right)\right), \tag{6}$$

where ρ_{r} is the receiving lens radius and η_0 is a constant empirical factor accounting for miscellaneous losses, such as detector inefficiency, which we ignore as illustrated above. In the downlink transmission, the loss model does not include air turbulence loss, and therefore we use the ideal Gaussian beam width as w_{LT} with Eq. (6) in the efficiency calculation.

B. Inter-Satellite Photon Transmission

As illustrated in Fig. 2, the end-to-end entanglements can be established through multiple satellites. When the incoming photon arrives, it first passes through the receiving lens, which focuses the diverged beam onto an optical element. The collimating lens then reshapes the refocused beam to a close-to-parallel beam, which effectively reduces beam divergence, thereby making it more robust against diffraction loss in the later propagation. After the collimation, the beam will be sent toward the next satellite. This segment forms a continuous optical path through multiple satellites, with each satellite receiving the incoming beam, collimating it, and forwarding it to the next node. The beam waist evolves throughout this process, and the transmission efficiency at each stage depends on the accumulated diffraction loss and collimation quality.

Beam propagation between satellite j and k: We begin with the propagation phase between two adjacent satellites j and k, such as satellites 1 and 2 in Fig. 2. Assume the beam waist of this relayed beam from SAT j (called incoming beam) is w_j, and it propagates through open space and finally reaches the receiver lens at SAT k with width $w_{j\to k}$ given by

$$(w_{j\to k})^2 = w_j^2\left(1+\left(\frac{L_{jk}}{z_{\mathrm{R}_j}}\right)^2\right), \tag{7}$$

where L_{jk} is the propagation distance between w_j and SAT k and $z_{\mathrm{R}_j} = \frac{\pi w_j^2}{\lambda}$ is the Rayleigh range of the incoming beam. Then the propagation efficiency between SAT j and SAT k, $\eta_{\mathrm{prop}}^{j\to k}$, is defined as how much light the receiving lens at SAT k could receive from w_j, given by

$$\eta_{\mathrm{prop}}^{j\to k} = 1-\exp\left(-2\left(\frac{\rho_{\mathrm{r}}}{w_{j\to k}}\right)^2\right). \tag{8}$$

Beam refocusing at satellite k: Upon arrival at satellite k, the incoming beam passes through a receiving lens, which acts to refocus the expanded beam. This step reduces the beam divergence accumulated during propagation and prepares it for the next stage of collimation, forming a new Gaussian beam with a beam waist w_k' inside the SAT k [23]

$$(w_k')^2 = w_j^2\frac{(f_{\mathrm{r}})^2}{(L_{jk}-f_{\mathrm{r}})^2+z_{\mathrm{R}_j}^2}, \tag{9}$$

where f_{r} is the focal length of the receiving lens. Note that when the propagation distance is much greater than the Rayleigh range (i.e. $L_{jk}\gg z_{\mathrm{R}_j}$), we assume the light beam captured by the receiving lens has a constant wave front [10]. The refocused beam forms an Airy disk located at one focal length away from the lens, with central disk width w_{Airy} [6]

$$w_k' = w_{\mathrm{Airy}} = \frac{1.22\lambda f_{\mathrm{r}}}{2\rho_{\mathrm{r}}}. \tag{10}$$

Since most of the light energy is contained within its central disk, whose pattern is similar to a Gaussian profile, we assume that this beam will propagate as a Gaussian beam with beam waist $w_k' = w_{\mathrm{Airy}}$ [10]. Notice that this constant-wave-front approximation also applies to the first refocused beam from uplink (inside SAT 1 in Fig. 2), as the beam has undergone a huge broadening effect due to turbulence.

Collimating and forwarding: After refocusing, the beam is sent through a collimating lens to minimize divergence for the next propagation segment. This completes one inter-satellite transmission cycle. The resulting beam waist and propagation state at the output of satellite k are then used as the input to the subsequent propagation phase toward satellite $k+1$. To collimate this refocused beam w_k' and relay it to the next satellite, the collimating lens should be placed one focal length away from the beam waist, producing a collimated beam on the opposite side, with waist width w_k, given by [1]

$$w_k = w_k'\frac{f_{\mathrm{c}}}{z_{\mathrm{R}_{k'}}}, \tag{11}$$

where f_{c} is the focal length of the collimating lens and $z_{\mathrm{R}_{k'}}$ is the Rayleigh range of the refocused beam w_k' inside SAT k.

The collimating efficiency at SAT k, η_{coll}^k, is given by

$$\eta_{\mathrm{coll}}^k = 1-\exp\left(-2\left(\frac{\rho_{\mathrm{c}}}{w_{k\to \mathrm{c}}'}\right)^2\right), \tag{12}$$

where $w_{k\to\mathrm{c}}'$ is the beam width when w_k' propagates to the collimating lens following the ideal Gaussian beam propagation, and ρ_{c} is the collimating lens' radius.

The inter-satellite link efficiency η^{jk} (from w_j to w_k) is

$$\eta^{jk} = \eta_{\mathrm{prop}}^{j\to k}\eta_{\mathrm{coll}}^k. \tag{13}$$

Summary: Assuming there are in total d satellites in a path, by iteratively applying this model across all satellites in the path, the total satellite-to-satellite transmission efficiency is

$$\eta_{\mathrm{ss}} = \prod_{i=1}^{d-1}\eta^{12}\eta^{23}...\eta^{(d-1)d}. \tag{14}$$

The overall end-to-end transmission efficiency between two ground stations s and t is:

$$\eta_{st} = \eta_{\mathrm{gs}}\eta_{\mathrm{ss}} = \eta_{\mathrm{gs}}\prod_{i=1}^{d-1}\eta^{12}\eta^{23}...\eta^{(d-1)d}. \tag{15}$$

The end-to-end loss is primarily affected by all distances between consecutive nodes along the paths, either between two satellites or between a satellite and a ground station, which can be represented as $Loss(st) = -10\log_{10}\eta_{st}$.

V. LACE: Loss-Aware Constellation Design

A. Problem Formulation

Based on the loss model described in the previous section, we now consider the problem of entanglement distribution between pairs of ground stations through a satellite network. Each such pair, denoted by st, is referred to as a source and destination (SD) pair, and the set of all SD pairs is denoted by U. Our objective is to design the satellite constellation in a way that minimizes the worst-case total transmission loss among all SD pairs. We formalize this in the following problem definition:

Definition 1 (LACE)**.** *Given the set of SD pairs U. The **Loss Aware Constellation Design** problem seeks to determine the constellation parameters $(\mathcal{P},\mathcal{N},h)$, which define the resulting*

Algorithm 1: End-to-end loss estimation algorithm

Input: Satellite graph $G = (V, E)$, SD pair st, visible satellite set V_s, V_t, initial beam width w_0
Output: Loss(st)

1 $vis(v) \leftarrow 0, pa(v) \leftarrow \perp, \text{Loss}(v) \leftarrow \infty, \forall v \in V \setminus V_s$;
2 $\text{Loss}(v) \leftarrow 0, \text{beam}(v) \leftarrow w_0, \forall v \in V_s$;
3 **while** *there exists unvisited node* **do**
4 $\quad v \leftarrow \arg\min_{v \in V}\{\text{Loss}(v) \mid vis(v) = 0\}$;
5 $\quad vis(v) \leftarrow 1$;
6 $\quad$ **if** v *is satellite sink in* V_t **then** break;
7 $\quad$ **for** $u \in$ *Neighbors*(v) **do**
8 $\quad\quad$ **if** $u \in V_s$ **then**
9 $\quad\quad\quad \text{Loss}(v) \leftarrow$ uplink loss using Eq. (6);
10 $\quad\quad\quad \text{beam}(v) \leftarrow$ refocused beam in Eq. (10);
11 $\quad\quad$ **else**
12 $\quad\quad\quad$ **if** $u \in V_t$ **then**
13 $\quad\quad\quad\quad \text{Loss}(vu) \leftarrow$ downlink loss using Eq. (6);
14 $\quad\quad\quad$ **else**
15 $\quad\quad\quad\quad \text{beam}(u) \leftarrow$ collimated beam in Eq. (11);
16 $\quad\quad\quad\quad \text{Loss}(vu) \leftarrow$ inter-satellite loss using Eq. (13);
17 $\quad\quad\quad$ **if** *Loss*$(u) >$ *Loss*$(v) +$ *Loss*(vu) **then**
18 $\quad\quad\quad\quad \text{Loss}(u) \leftarrow \text{Loss}(v) + \text{Loss}(vu)$;
19 $\quad\quad\quad\quad pa(u) \leftarrow v$;
20 **return** *Loss*(st);

satellite network $G = (V, E)$, such that the maximum total loss over all SD pairs in U is minimized, which is:

$$\min_{(\mathcal{P},\mathcal{N},h)} \max_{st \in \mathcal{U}} \textit{Loss}(st \mid \mathcal{P}, \mathcal{N}, h)$$

where Loss(st) denotes the end-to-end loss of pair st. Given a specific constellation decided by $(\mathcal{P}, \mathcal{N}, h)$, the ISLs are typically connected in a fixed manner among all satellites. Thus, the satellite network and the GSLs are uniquely defined for a specific time based on the satellites' locations. This objective is subject to the following design constraints.

(1) Full ground station coverage: At any time, each ground station must have at least one satellite above $\theta_{\min}$. This constraint ensures that any ground station pair can send photons to or receive photons from the satellite network at any time.

(2) Satellite numbers constraint: To reflect physical limitations, we impose an upper bound $\mathcal{V}$ on the total number of satellites. Specifically, given a constellation with $\mathcal{P}$ orbital planes, and $\mathcal{N}$ satellites per orbit, it is required that $\mathcal{P} \times \mathcal{N} \leq \mathcal{V}$.

B. End-to-end Loss Estimation Algorithm Design

To solve the LACE problem, we estimate the total loss under a given constellation configuration. This requires, for each SD pair $st \in U$, identifying a feasible transmission path through the satellite network and computing its total loss based on the propagation loss model. Since the loss over an inter-satellite link depends on the cumulative beam evolution from the source, the loss along a path is not a simple sum of independent link losses. Instead, it must be computed sequentially along the path, with the beam width dynamically updated at each hop.

Algorithm 1 is to estimate the end-to-end loss for an SD pair st. Line 1 and Line 2 initialize visited flag $vis(\cdot)$, the parent node $pa(\cdot)$, the initial loss Loss$(\cdot)$ and beam width beam$(\cdot)$ for all satellites in graph. In each iteration, the algorithm starts from the node with the least loss and then marks it as visited in Lines 3–5. In Lines 7–16, the algorithm updates the loss for neighboring nodes and checks if the newly computed path provides a lower cumulative loss compared to previous records. Unlike traditional Dijkstra's algorithm where each edge has a static, independent loss, here the path loss dynamically evolves along the path based on the evolution of light beam. Specifically, after each hop, the beam waist and propagation distance are updated based on the loss model, affecting the efficiency and thus the loss of subsequent links. Consequently, a node with a smaller cumulative loss at the current hop does not guarantee a lower loss after additional hops, as the degradation of beam state may lead to higher losses of the next hop. This interdependence between the beam evolution and path loss accumulation requires careful updating of the beam state along with the loss at each node. The algorithm ends when all nodes are visited. For the time complexity, since the number of satellites is $|V|$ and the number of edges is $|E|$, the algorithm runs in $O(|E|+|V| \log |V|)$ time using a Fibonacci heap, where $|E| = O(|V|)$ for typical satellite network topologies.

Algorithm 2: LACE Constellation Design Framework

Input: Total number of satellites $\mathcal{V}$, inclination angle i, minimum elevation angle $\theta_{\min}$, SD pairs $\mathcal{U}$
Output: Constellation $(\mathcal{P}', \mathcal{N}', h')$

1 $\text{Loss}_{\min} \leftarrow \infty$, $(\mathcal{P}', \mathcal{N}', h') \leftarrow (\perp, \perp, \perp)$;
2 Get all valid constellation configuration set in $\mathcal{V}$;
3 **for** *valid constellation configuration set* $(\mathcal{P}, \mathcal{N}, h)$ **do**
4 $\quad$ **for** *each time interval* $T \in \mathbf{T}$ **do**
5 $\quad\quad$ Build satellite network graph G with parameters $(\mathcal{P}, \mathcal{N}, h)$ and inclination i;
6 $\quad\quad$ **for** *each st pair in* $\mathcal{U}$ **do**
7 $\quad\quad\quad$ Identify visible satellites V_s, V_t (Eq. (1));
8 $\quad\quad\quad$ **if** $V_s \neq \emptyset \cap V_t \neq \emptyset$ **then**
9 $\quad\quad\quad\quad$ Call Algorithm 1 to get Loss(st);
10 $\quad\quad\quad$ **if** *Loss*$(st) <$ *Loss*$_{min}$ **then**
11 $\quad\quad\quad\quad$ Update $\text{Loss}_{\min} \leftarrow \text{Loss}(st)$;
12 $\quad\quad\quad\quad \mathcal{P}' \leftarrow \mathcal{P}$, $\mathcal{N}' \leftarrow \mathcal{N}$, $h' \leftarrow h$;
13 **return** *constellation* $(\mathcal{P}', \mathcal{N}', h')$

C. LACE Constellation Design Framework

Based on the loss model and our end-to-end loss algorithm design, the LACE framework is shown in Algorithm 2. Given a total number of satellites $\mathcal{V}$ and inclination angle i, the algorithm will first find all combinations of $\mathcal{P}$ and $\mathcal{N}$ whose product is equal to $\mathcal{V}$ in Line 2. The details of this enumeration process and its practical considerations are discussed later in this section. Then, the algorithm checks all feasible combinations in Line 3 and constructs a satellite network $G = (V, E)$. In Lines 4–12, the algorithm estimates the end-to-end loss at every time interval if there exist visible satellites for ground stations st. The algorithm compares all end-to-end losses for different constellations and returns the final feasible constellation. The overall time complexity is $O(|\mathcal{C}| \cdot |\mathcal{U}| \cdot \mathbf{T} \cdot L)$, where $|\mathcal{C}|$ is the

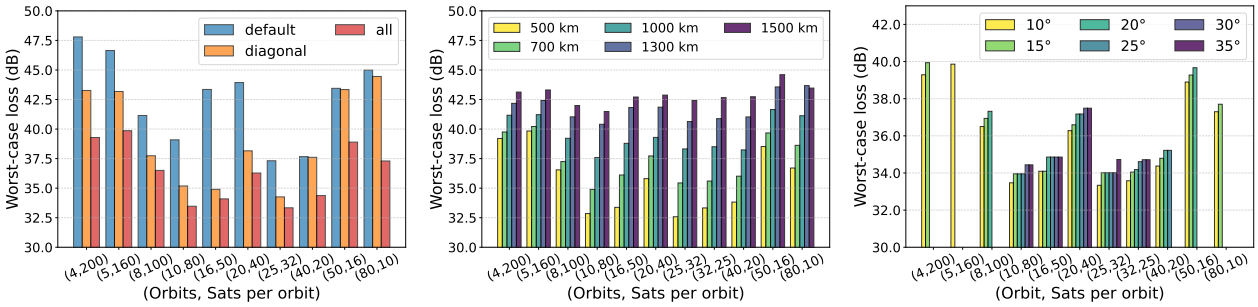

(a) Impact of link connectivity (b) Impact of altitude (c) Impact of elevation angle

Fig. 3: Worst-case loss in average for a fixed number of satellites

number of valid constellation configurations, $|\mathcal{U}|$ is the number of SD pairs, $\mathbf{T}$ is the total number of time intervals considered and L is the time to estimate the end-to-end loss in Alg. 1.

VI. Evaluation Results

A. Evaluation Methodology

We simulated an LEO satellite constellation with the furthest ground station pair located in major cities around the world. By evaluating the loss for the farthest pair, we capture the worst-case behavior of the network under realistic orbital dynamics. The distances between the ground stations were calculated using the longitude and latitude provided in [16]. The plane inclination was 90 degrees. The default total number of satellites was 800, the default altitude was 550 km, and the minimum elevation angle was set to be 10 degrees. The constellation provided seamless coverage of ground stations at any time. For our loss model, the parameters related to optical beam propagation and lens characteristics were defined as follows [4], [10]. We assume that all the lenses (both receiving and collimating) on all satellites share the same fixed size (ρ) and focal length (f) as 1 m. We set wavelength (λ) as 810 nm and the initial beam divergence angle as 15 μrad for calculating the initial beam waist $w_0 = \frac{\lambda}{\pi \cdot \theta_{\text{div}}}$. Additionally, for accurately modeling line-of-sight constraints, we set R_{e} as 6371 km.

We examined three distinct ISL connection strategies: (1) **Default:** we adopt the widely utilized +Grid topology, in which each satellite forms links with its two immediate neighbors within the same orbit and one nearest satellite in each adjacent orbit, resulting in four ISLs per satellite. (2) **Diagonal:** each satellite connects to all feasible satellites in adjacent planes, establishing links wherever direct line-of-sight is available and not obstructed by the Earth. (3) **All:** each satellite establishes ISLs with all other satellites within its line-of-sight. To determine whether Earth obstructs an ISL, we computed the midpoint of the link in the ECEF coordinate system. The altitude of this midpoint is obtained by subtracting Earth's radius from its Euclidean norm. The link is considered feasible if the altitude is positive. We monitored GSL changes every 10 seconds. Results were averaged over 3 runs in the same setting. We used ***worst-case loss in average*** to measure the average end-to-end loss of the farthest SD pair over time.

B. Evaluation Results

1) Worst-case loss comparison: Fig. 3 shows the worst-case loss across various combinations while maintaining a fixed bound of 800 on the total number of satellites. We observe that the network using "all" maintains the lowest loss across different combinations in Fig. 3(a). This result highlights that equipping satellites with a sufficient number of lenses provides greater flexibility in establishing ISLs. Moreover, configurations where satellites are more evenly distributed tend to reduce end-to-end loss, compared to highly imbalanced deployments. Additionally, even when employing the "all", orbital altitude and elevation angle continue to have a notable impact on the overall transmission loss. In Fig. 3(b), the worst-case loss increased as altitude increased. This indicates that deploying satellites at higher altitudes results in increased uplink and downlink distances, as well as longer inter-satellite link distances, thereby significantly elevating the total loss. In Fig. 3(c), as the elevation angle increased, the number of satellites visible to ground stations correspondingly decreased, reducing the availability of feasible paths and potentially resulting in situations where no entanglements can be established. Thus, our first key observation is **dense and balanced distributed satellites with sufficient lenses and moderate altitudes are critical for minimizing total transmission loss.**

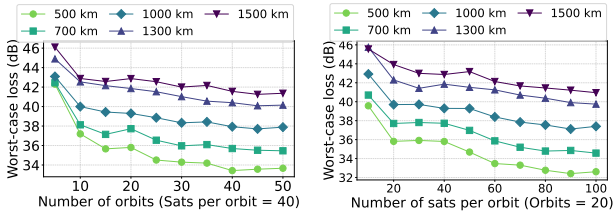

(a) Number of orbits (b) Number of satellites/orbit

Fig. 4: Worst-case loss in average at different altitudes

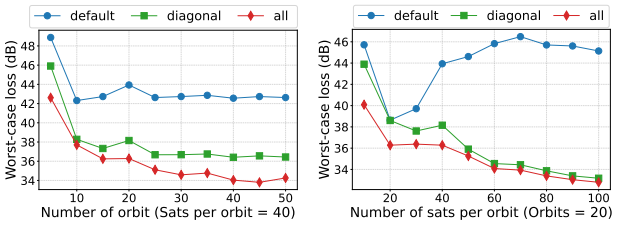

(a) Number of orbits (b) Number of satellites/orbit

Fig. 5: Worst-case loss in average in different link connections

2) Different altitudes comparison: Fig. 4 shows the worst-case loss at different altitudes. The loss decreased with the increasing number of orbits in Fig. 4(a) and with the increasing number of satellites per orbit in Fig. 4(b). We observe that

increasing the number of orbital planes or satellites per orbit consistently reduces the end-to-end. Furthermore, lower orbital altitudes (e.g., 500 km) yield significantly reduced losses compared to higher altitudes (e.g., 1500 km), reflecting the increased transmission distances involved at higher altitudes. Our second key observation is **careful selection of configuration, specifically increasing orbital density and reducing altitude, can effectively enhance the performance of distribution.**

3) Different link connection comparison: Fig. 5 shows the worst-case loss at different link connections. As in Fig. 5(a), the loss initially decreased significantly as the number of orbital planes increased. However, beyond approximately 25 orbital planes, the reduction in loss became marginal, and the curve gradually flattened. This observation indicates diminishing returns from further increasing the number of orbital planes, suggesting that deploying redundant orbital planes may not yield substantial additional benefits in terms of loss reduction. As in Fig. 5(b), the loss using "all" and "diagonal" decreased with the increase of the number of satellites per orbit, which indicates that the increasing number of satellites per orbit can provide more feasible lightpaths and further decrease the end-to-end loss. However, the loss using "default" first decreased and then increased with the increasing number of satellites per orbit. This is because each satellite in "default" can establish ISLs only in four directions. Consequently, when the number of satellites per orbit increases, the establishment of entanglement paths between distant ground stations typically requires more intermediate hops, particularly involving satellites within the same orbit. These additional hops lengthen the overall entanglement path, thereby increasing the cumulative photon loss. Our third key observation is **increasing the number of planes and satellites per orbit generally reduces total loss, but excessive orbital planes yield diminishing returns, and limited ISL connectivity like +Grid suffers increased loss at high satellite densities due to longer multi-hop paths.**

To summarize, **LACE can serve as a guide for building a global-scale satellite-assisted quantum internet with a complete ISL connection strategy.**

VII. Conclusion

In this paper, we introduced a Loss-Aware Constellation Design framework (LACE) for satellite-based passive optical quantum networks. aimed at enabling global-scale entanglement distribution. By developing a comprehensive beam propagation loss model that incorporates diffraction, turbulence, and beam truncation, we provided an accurate foundation for evaluating end-to-end photon loss. We further propose an algorithm to estimate the loss for end-to-end entanglements and also develop a constellation design framework to determine the constellation parameters. Through extensive simulations across diverse constellation settings, we demonstrate how key orbital and topological parameters influence transmission loss, offering valuable insights for large-scale quantum network design.

References

[1] "Collimated Light's Non-Zero Beam Divergence," accessed 2025-05-05. URL: https://www.thorlabs.com/newgrouppage9.cfm?objectgroup_id=14489

[2] L. Andrews, R. Phillips, and P. Yu, "Optical scintillations and fade statistics for a satellite-communication system," *Applied Optics*, vol. 34, no. 33, pp. 7742–7751, 1995.

[3] C. H. Bennett and G. Brassard, "Quantum cryptography: Public key distribution and coin tossing," *Theoretical Computer Science*, 2014.

[4] C. Bonato, A. Tomaello, V. Da Deppo, G. Naletto, and P. Villoresi, "Feasibility of satellite quantum key distribution," *New Journal of Physics*, vol. 11, no. 4, p. 045017, 2009.

[5] K. Boone, J.-P. Bourgoin, E. Meyer-Scott, K. Heshami, T. Jennewein, and C. Simon, "Entanglement over global distances via quantum repeaters with satellite links," *Physical Review A*, vol. 91, no. 5, p. 052325, 2015.

[6] M. Born and E. Wolf, *Principles of optics: electromagnetic theory of propagation, interference and diffraction of light*. Elsevier, 2013.

[7] C. Cicconetti, M. Conti, and A. Passarella, "Resource allocation in quantum networks for distributed quantum computing," in *IEEE SMARTCOMP*, 2022, pp. 124–132.

[8] R. Deng, B. Di, H. Zhang, L. Kuang, and L. Song, "Ultra-dense leo satellite constellations: How many leo satellites do we need?" *IEEE Transactions on Wireless Communications*, vol. 20, no. 8, pp. 4843–4857, 2021.

[9] F. Dios, J. A. Rubio, A. Rodríguez, and A. Comerón, "Scintillation and beam-wander analysis in an optical ground station-satellite uplink," *Applied Optics*, vol. 43, no. 19, pp. 3866–3873, 2004.

[10] S. Goswami and S. Dhara, "Satellite-relayed global quantum communication without quantum memory," *Physical Review A*, vol. 20, no. 2, p. 024048, 2023.

[11] H. Gu, Z. Li, R. Yu, X. Wang, F. Zhou, J. Liu, and G. Xue, "Fendi: Toward high-fidelity entanglement distribution in the quantum internet," *IEEE/ACM Transactions on Networking*, 2024.

[12] H. Gu, R. Yu, Z. Li, X. Wang, and G. Xue, "Quesat: Satellite-assisted quantum internet for global-scale entanglement distribution," *IEEE INFOCOM*, 2025.

[13] J. W. Hardy, *Adaptive optics for astronomical telescopes*. Oxford university press, 1998, vol. 16.

[14] M. Hein, W. Dür, and H.-J. Briegel, "Entanglement properties of multipartite entangled states under the influence of decoherence," *Physical Review A*, vol. 71, no. 3, p. 032350, 2005.

[15] Y. Huang, F. Salces-Carcoba, R. X. Adhikari, A. H. Safavi-Naeini, and L. Jiang, "Vacuum beam guide for large scale quantum networks," *Physical Review Letters*, vol. 133, no. 2, p. 020801, 2024.

[16] B. S. Kempton, *A simulation tool to study routing in large broadband satellite networks*. Christopher Newport University, 2020.

[17] S. Khatri, A. J. Brady, R. A. Desporte, M. P. Bart, and J. P. Dowling, "Spooky action at a global distance: analysis of space-based entanglement distribution for the quantum internet," *npj Quantum Information*, vol. 7, no. 1, p. 4, 2021.

[18] P. G. Kwiat, K. Mattle, H. Weinfurter, A. Zeilinger, A. V. Sergienko, and Y. Shih, "New high-intensity source of polarization-entangled photon pairs," *Physical Review Letters*, vol. 75, no. 24, p. 4337, 1995.

[19] X. Li, P. L. Voss, J. E. Sharping, and P. Kumar, "Optical-fiber source of polarization-entangled photons in the 1550 nm telecom band," *Physical Review Letters*, vol. 94, no. 5, p. 053601, 2005.

[20] S.-K. Liao, W.-Q. Cai, W.-Y. Liu, L. Zhang, Y. Li, J.-G. Ren, J. Yin, Q. Shen, Y. Cao, Z.-P. Li *et al.*, "Satellite-to-ground quantum key distribution," *Nature*, vol. 549, no. 7670, pp. 43–47, 2017.

[21] N. K. Panigrahy, P. Dhara, D. Towsley, S. Guha, and L. Tassiulas, "Optimal entanglement distribution using satellite based quantum networks," in *IEEE INFOCOM WKSHPS*, 2022, pp. 1–6.

[22] S. Pirandola, R. Laurenza, C. Ottaviani, and L. Banchi, "Fundamental limits of repeaterless quantum communications," *Nature Communications*, vol. 8, no. 1, p. 15043, 2017.

[23] S. A. Self, "Focusing of spherical gaussian beams," *Applied Optics*, vol. 22, no. 5, pp. 658–661, 1983.

[24] G. C. Valley, "Isoplanatic degradation of tilt correction and short-term imaging systems," *Applied Optics*, vol. 19, no. 4, pp. 574–577, 1980.

[25] W. K. Wootters and W. H. Zurek, "A single quantum cannot be cloned," *Nature*, vol. 299, no. 5886, pp. 802–803, 1982.

[26] J. Yin, Y. Cao, Y.-H. Li, S.-K. Liao, L. Zhang, J.-G. Ren, W.-Q. Cai, W.-Y. Liu, B. Li, H. Dai *et al.*, "Satellite-based entanglement distribution over 1200 kilometers," *Science*, vol. 356, no. 6343, pp. 1140–1144, 2017.

[27] Z. Zhang, C. You, O. S. Magaña-Loaiza, R. Fickler, R. d. J. León-Montiel, J. P. Torres, T. S. Humble, S. Liu, Y. Xia, and Q. Zhuang, "Entanglement-based quantum information technology: a tutorial," *Advances in Optics and Photonics*, vol. 16, no. 1, pp. 60–162, 2024.

[28] Z. Zhang and Q. Zhuang, "Distributed quantum sensing," *Quantum Science and Technology*, vol. 6, no. 4, p. 043001, 2021.